Indian Journal of Chemistry
Vol. 57A, Aug-Sept 2018, pp. 1121-1127

Dicyanomethylene substituted oxocarbon dianions: A comparative computational study

Promila, Anuj Tripathi & Chetti Prabhakar*
Department of Chemistry, National Institute of Technology, Kurukshetra 136 119, India
Email: chetty_prabhakar@yahoo.com

Received 30 April 2018; revised and accepted 30 July 2018

A comparative and computational study of various dicyanomethylene substituted dianions of squarate (SQ1-SQ3), croconate (CR1-CR4) and rhodizonate (RH1-RH7) with absorption in the visible to the near-infrared region (300-800 nm) is reported. Rhodizonate dianions show ~100 nm red-shifted absorption as compared to corresponding croconate dianions. Similarly, croconate dianions show ~100 nm red-shifted absorption as compared to the corresponding squarate dianions. Further, on increasing the number of dicyanomethylene substitutions on the central ring, there is a change in electronic properties (absorption shifts toward longer wavelength). The drastic changes in absorption properties are due to the variation in size of the central ring as shown by DFT, TDDFT and SAC-CI data.

Keywords*:* Theoretical chemistry, Electronic properties, Oxocarbon dianions, Dicyanomethylene, Squarate, Croconate, Rhodizonate

Oxocarbon acids are one of the most important class of organic molecules with the general formula $H_n(C_nO_n)$, where, n = 3 for deltic acid, 4 for squaric acid, 5 for croconic acid and 6 for rhodizonic acid. The corresponding dianions $(C_nO_n)^{2-}$ known as oxocarbon dianions. Oxocarbon dianions are generally called deltate, squarate, croconate and rhodizonate dianions with n = 3, 4, 5 and 6 respectively (Scheme 1). This class $[(C_3O_3)^{2-}$ $(C_4O_4)^{2-}$, $(C_5O_5)^{2-}$ and $(C_6H_6)^{2-}]$ of organic molecules along with their electronic properties was first examined by West and co-workers in 1960[1]. These dianions have interesting spectroscopic properties due to the delocalized electronic structure over the oxocarbon ring and then high molecular symmetry[2-6]. Also, these molecules have a planar structure with D_{nh} symmetry as revealed by Raman and IR spectroscopic analysis[7, 8] and further confirmed by X-rays diffraction studies[9,10]. Due to large π-electron delocalization, the oxocarbon anions show strong absorption in the UV and visible regions, except for the deltate derivative, which is expected to absorb at ~200 nm[11] lower wavelength as compared to the other derivatives. Oxocarbons, where the oxygen atom of carbonyl group is partially or completely replaced by sulphur, selenium, dicyanomethylene or by other groups, lead to the formation of derivatives called pseudo-oxocarbons[12-13]. Oxocarbon and pseudo-oxocarbon molecules can be involved in different types of intermolecular interaction, where electronic delocalization provides the possibility of π-stacking interaction between rings. Further, these molecules have coordination properties and acceptor sites for hydrogen bonding which make this system potentially useful in crystal engineering research.

The interesting fundamental chemical aspects of these molecules have motivated many studies on their optoelectronic properties[7-13]. Rhodizonic acid is used as an analytical reagent for Fe, Pb and Ba[14] while squaric acid derivatives are involved in some biochemical and photoconductive processes. Generally, the oxocarbons are used as photoreceptors[12].

The 1, 2 and 1, 3 bis(dicyanomethylene) substituted squarate dianions have high molecular symmetry and smaller molecular size than the next higher oxocarbon dicyanomethylene derivative croconate dianion[15,16]. Condensation reaction between croconic acid and malononitrile ($NCCH_2CN$) results in the formation of interesting dianions, viz., croconate blue (2,4,5-tris(dicyanomethylene)cyclopentene-1,3-dionate[15], where three non-adjacent oxygens atoms are replaced by dicyanomethylene group) and croconate violet (3,5-bis(dicyanomethylene) cyclopentane-1,2,4-trionate[16], where two non-adjacent oxygens are replaced by dicyanomethylene group). These molecules have a relatively short backbone that is easy to synthesize and to carry out structural variation to tune the absorption, emission and thermal stability, which makes them good materials for various optoelectronic applications. These molecules show interesting properties such as typical semiconductor properties, intense colour, higher π-electron delocalization expressing strong absorption bands in the visible region, reversible electrochemical behavior and photophysical properties and hence find application in supramolecular chemistry[17-19]. The synthesis of the next higher analog of croconate (i. e., rhodizonate) dianion with dicyanomethylene is still a challenging task.

In our earlier reports, we performed DFT studies on visible to near infrared absorbing squaraines and croconines and found that there is good agreement between experimental and theoretical results[20]. It was also observed that with an increase in the size of central acceptor ring there was a change in electronic properties (absorption). In continuation herein, we extend the study to dicyanomethylene substituted oxocarbon dianions. To the best of our knowledge, in literature there are very few reports available on rhodizonates. Herein we have performed a comparative computational study of dicyanomethylene substituted derivatives of squarate, croconate, and rhodizonate dianions and compared their electronic excitations with available experimental results[15, 21, 22].

Our main aim is to study the effect of size of neutral dianion ring on the absorption maxima (effect of the central ring). Further, we have also studied the effect of increase in the number of substituents (i.e., dicyanomethylene group) on central ring. For this we considered fourteen molecules (Scheme 2); three are derivatives of squarate dianions (SQ1, SQ2, and SQ3), four are croconate dianion derivatives (CR1, CR2, CR3, and CR4) and seven are rhodizonate dianion derivatives (RH1, RH2, RH3, RH4, RH5, RH6, and RH7), with dicyanomethylene group(s) substitution on the central moiety. Among these fourteen molecules, four molecules (SQ2, SQ3, CR3, and CR4) are reported experimentally and remaining are to be synthesized. We have compared the experimental absorption values with theoretically calculated absorption energies in SQ and CR. On the basis of good correlation between the calculated and experimental excitations in SQ and CR, we have also reported the electronic properties of different rhodizonate dianions.

Computational Methods

All the molecules in Scheme 2 are optimized by using the Gaussian 09W quantum chemical package[23]. The minima energy search for all dianion molecules was carried out using the Becke's three-parameter hybrid exchange functional and the Lee-Yang-Parr correlation functional (LYP) with a 6-311+G(d, p) basis set[24,25]. No symmetric restrictions were imposed during energy minimization for all the molecules. True minima were characterized from frequency analysis and frequencies were evaluated for the optimized geometries at the same level of calculations. To predict the absorption spectrum, lowest five singlet excitation energies were calculated using the TDDFT methodology with 6-311+G (d, p) basis set. Symmetry adopted cluster- configuration interaction (SAC-CI) calculations were carried out with 6-31+G(d) basis set. Frontier molecular orbitals were responsible for the electronic excitation leading to absorption maxima visualized from the population analysis carried out at B3LYP/6-311+ G (d, p) level.

Results and Discussion

Linear optical properties (Electronic excitation)

The experimentally reported absorption maxima for SQ2 (1, 2-disubstituted squarate dianion) is 381 nm and that for SQ3 (1,3-disubstituted squarate dianion) is 423 nm. There is a ~40 nm difference between SQ2 and SQ3[22]. The red-shift in the case of SQ3 is due to more effective electron transfer as compared to SQ2. In the case of croconate dianion, the CR3 (1,3-disubstituted croconate dianion) shows absorption at 533 nm[21], while the CR4 (trisubstituted croconate dianion) shows absorption at 599 nm[15]. This red shift in absorption from CR3 to CR4 is due to the increase in number of dicyanomethylene groups on the central five-member ring and more effective electron transfer in CR4. From TDDFT calculations, the calculated absorption maxima for SQ1 (monosubstituted squarate dianion) and SQ2 (1,2-disubstituted squarate dianion) are at 321 nm and 346 nm respectively. SQ2 shows higher absorption than SQ1, due to increase in conjugation and increase in number of dicyanomethylene groups on the central four-membered ring. On moving from SQ2 to SQ3, a red-shift of 50 nm was observed even though both are disubstituted squarate dianions (differing only in the position of substitution of dicyanomethylene group) and are in good agreement with the experimentally reported absorption energies. An overall red-shift of 80 nm was observed on moving from SQ1 to SQ3. This is due to more efficient charge transfer and increase in the number of dicyanomethylene groups

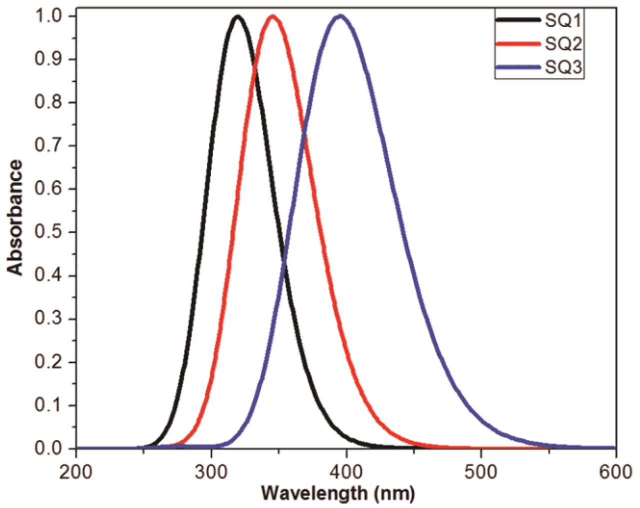

Fig. 1 — Calculated absorption spectra for squarate dianion derivatives (SQ1-SQ3).

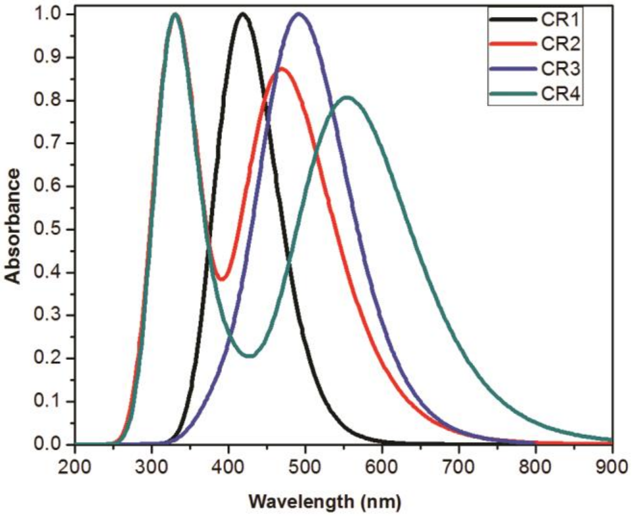

Fig. 2 — Calculated absorption spectra for croconate dianion derivatives (CR1-CR4).

Table 1 — Calculated absorption maxima (λ_{max}, nm), oscillator strength (*f*), major transitions (MT), configurations of greater contributions (%C_i) for SQ1-SQ3, CR1-CR4 and RH1-RH7 dianions in gas phase at TD-B3LYP/6-311+G(d, p) method for B3LYP/6-311+G(d, p) optimized geometries

Molecule	λ_{max} (Expt.)	λ_{max} (Calc.)	*f*	MT	C_i (%)
SQ1		321	0.459	H→L	98
SQ2	381[a]	346	0.432	H→L	97
SQ3	423[a]	395	0.786	H→L	98
CR1		418	0.462	H→L	96
CR2		486	0.113	H-1→L	59
CR3	533[b]	493	0.630	H→L	98
CR4	599[c]	565	0.277	H→L	93
RH1		521	0.371	H→L	88
RH2		587	0.047	H-1→L	55
RH3		603	0.455	H→L	97
RH4		621	0.563	H→L	97
RH5		654	0.296	H→L	94
RH6		665	0.391	H→L	95
RH7		739	0.087	H→L	85

[a]Ref. 22; [b]Ref. 21; [c]Ref. 15.

in the squarate dianion. The TDDFT calculated absorption spectra of squarate dianions (SQ1-SQ3) are shown in Fig. 1. The calculated absorption spectra, oscillator strength, and corresponding orbital transitions are shown in Table 1.

A similar trend is followed in the case of the croconate series with an increase in the number of dicyanomethylene groups on the central five-membered ring (Fig. 2). On moving from CR1 to CR2, almost 70 nm red-shift absorption was observed. This red-shifted absorption is due to the increase in conjugation and increase in the number of dicyanomethylene groups on the central five-membered croconate ring. Both CR2 and CR3 are disubstituted derivatives and hence there is negligible difference in the absorption maxima (~7 nm) of two molecules. On further substitution of dicyanomethylene group on the croconate ring, i.e., molecule CR4, there is a further increase in the absorption maxima at 565 nm, which is 70 nm higher than CR3 (CR2) and 150 nm red-shifted than CR1. This is due to more efficient electron transfer and increase in the number of dicyanomethylene groups on the five-member ring in CR4. Hence, this red-shift is due to increase in the number of dicyanomethylene groups on central moiety as compared to CR1, CR2 and CR3. Absorption spectra for croconate dianions (CR1-CR4) are shown in Fig. 2.

Similar to squarate and croconate dianions, rhodizonate dianions follow the same trend of increase in absorption maxima with increase in the number of dicyanomethylene groups on the central ring. On moving from RH1 (monosubstitution on central acceptor ring) to RH3 (1, 3-dicyanomethylene substituted rhodizonate dianion), ~80 nm red-shifted absorption was observed. Due to more effective electron transfer in 1, 4-substituted rhodizonate dianion (RH4), a more red-shifted absorption was observed in RH4 as compared to RH3. From RH3 to RH6 (1, 2, 4-trisubstituted rhodizonate dianions), there is a red-shift of ~62 nm. The absorption spectra of rhodizonate dianions are shown in Fig. 3.

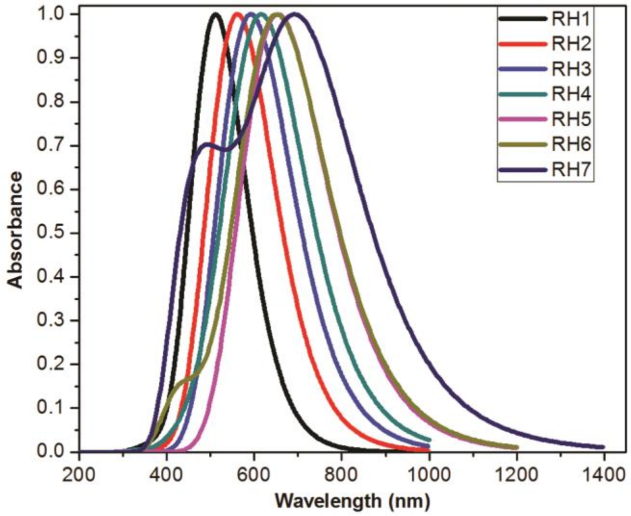

Fig. 3 — Calculated absorption spectra for rhodizonate dianion derivatives (RH1-RH7).

To rationalize the methodology, we performed DFT studies with different functionals such as B3LYP[25], M06[26], BHLYP[27] and with long range corrected functional CAM-B3LYP[28] and WB97XD[29]. B3LYP is global gradient corrected hybrid method with constant 25% Hartree-Fock (HF) exchange[25], while M06 is a global hybrid functional (hybrid meta GGA) with 27% HF exchange[26] and BH and HLYP (Becke-Half-and-Half-LYP) is 1:1 mixture of DFT method and exact exchange energies (50% HF exchange)[27]. CAM-B3LYP and WB97XD are range separated hybrid functional with short range HF exchange[28, 29]. The CAM-B3LYP (Coulomb attenuated version of B3LYP) functional comprises 19% HF exchange at short range and 65% HF exchange interaction at long range[28]. Similarly, WB97XD comprises 22% and 100% HF exchange at short range and long range respectively[29]. For all the calculations, 6-311+G(d, p) basis set was used to predict geometries of squarate, croconate and rhodizonate dianions. From the optimized structures, it was observed that there is no major change in geometry of the molecules (bond lengths and bond angles) with change in functionals. Bond lengths and bond angles calculated with different functionals for SQ3, CR3 and RH3 are tabulated in Table S1 (Supplementary Data). It is also evident from the literature; B3LYP functional are good for ions for predicting photophysical properties[30].

Further, to know the effect of different functionals on electronic excitations, we have carried out TD-DFT calculations for B3LYP optimized geometries for all the molecules using long-range functionals with CAM-B3LYP and WB97XD (Table 2), which are consistent with the results calculated at B3LYP in the SQ, CR series of molecules. There is hardly a difference of 10 nm with long-range functionals, but in the case of RH series, deviation up to 60 nm is observed with CAM-B3LYP and WB97XD long-range functionals as compared to B3LYP.

Table 2 — Calculated absorption maxima (λ_{max} in nm) and oscillator strength (f) for SQ1-SQ3, CR1-CR4 and RH1-RH7 in gas phase at TD-DFT/6-311+G(d, p) with different functionals for B3LYP/6-311+ G (d, p) optimized geometries

Molecule	B3LYP		CAM-B3LYP		WB97XD	
	λ_{max}	f	λ_{max}	f	λ_{max}	f
SQ1	321	0.459	315	0.003	310	0.541
SQ2	346	0.432	331	0.557	331	0.551
SQ3	395	0.786	390	0.865	391	0.854
CR1	418	0.462	422	0.525	427	0.508
CR2	486	0.113	494	0.125	505	0.107
CR3	493	0.630	504	0.710	515	0.695
CR4	565	0.277	554	0.376	563	0.372
RH1	521	0.370	540	0.465	552	0.450
RH2	587	0.047	572	0.312	582	0.304
RH3	604	0.455	631	0.531	652	0.519
RH4	621	0.563	660	0.635	682	0.623
RH5	654	0.296	663	0.382	686	0.373
RH6	665	0.391	687	0.488	708	0.481
RH7	739	0.087	708	0.137	724	0.129

Effect of basis set

To know the effect of basis set on the geometries and electronic excitations, we carried out calculations at B3LYP and TD-B3LYP method with different basis sets such as 6-311G(d, p), 6-31+G(d, p), 6-31++G(d, p), 6-311+G(d, p) and 6-311++G(d, p) for SQ3, CR3 and RH3. Geometrical parameters of the optimized geometries with various basis sets are shown in Table S2 (Supplementary Data) for SQ3, CR3 and RH3 respectively. Table S2 shows that there is minimal difference in the geometry of SQ3, CR3 and RH3 with the change in a basis set from polarized to diffused basis set with polarization. It is also clear that there is no change in the bond lengths and bond angles with the change in basis sets from triple zeta polarized basis set (6-311G(d, p)) to diffused triple zeta polarized basis set (6-311++G(d, p)). Further, to know the effect of these basis sets on absorption energies, TD-DFT calculations with different basis sets were carried out for SQ3, CR3 and RH3. There is no major difference in absorption maxima (~10 nm) with the change in basis sets as shown in Table 3. Hence, further studies were based on the 6-311+G(d, p) basis set.

Table 3 — Absorption energies (λ_{max}, nm) and oscillator strength (f) calculated at TD-B3LYP level with different basis sets for SQ3, CR3 and RH3 for B3LYP/6-311+G(d,p) optimized geometries

Basis set	SQ3		CR3		RH3	
	λ_{max}	f	λ_{max}	f	λ_{max}	f
6-311G(d,p)	387	0.734	486	0.581	607	0.456
6-31+G(d,p)	395	0.794	495	0.634	607	0.456
6-31++G(d,p)	395	0.794	495	0.634	604	0.455
6-311+G(d,p)	395	0.786	493	0.630	604	0.455
6-311++G(d,p)	395	0.786	493	0.630	598	0.420

Table 4 — HOMO, LUMO energies, HOMO-LUMO gap (HLG) and central C-C-C angle variations

Molecule	HOMO (eV)	LUMO (eV)	HLG (eV)	C1-C2-C3 (deg)[a]
SQ1	2.22	5.96	3.74	88.5
SQ2	1.30	5.09	3.79	88.4
SQ3	1.22	4.36	3.14	89.6
CR1	1.75	4.56	2.81	107.3
CR2	0.95	3.60	2.64	106.7
CR3	0.93	3.23	2.30	107.4
CR4	0.42	2.69	2.27	-
RH1	1.42	3.55	2.13	117.1
RH2	0.74	2.84	2.10	117.4
RH3	0.68	2.48	1.80	119.8
RH4	0.66	2.32	1.66	-
RH5	0.11	1.92	1.81	-
RH6	0.16	1.84	1.69	-
RH7	0.15	1.99	1.84	-

[a] Numbering as shown in Scheme 2.

Effect of change of central ring or central angle on absorption energies

To know the effect of the change in the central ring or central angle, we also studied the results calculated by TDDFT for dicyanomethylene substituted rhodizonate, croconate and squarate dianions. When the central four-member ring in squarate dianion (SQ3) was replaced with a five-member ring (CR3), the variation in central angle was ~20° and when the five-member ring was replaced with a six-member ring (RH3), an ~10° variation in central angle was observed with an increase in the central angle. The central angle variation is shown in Table 4.

The increase in absorption of rhodizonate dianions were correlated with squarate and croconate dianions by considering central the C-C-C angle variation (numbering shown in Scheme 2)[31-32]. The larger wavelength is correlated to the larger central C-C-C angle, which leads to smaller HLG. As we move from SQ1 (central four-member ring) to CR1 (central five-member ring), a red-shift of 100 nm occurs and from CR1 to RH1 (central six-member ring), a red-shift of more than 100 nm was observed even though all these have a similar substituent. The absorption spectra for SQ1, CR1 and RH1 are shown in Fig. 4. In a similar way, RH2 shows a red-shift of more than 100 nm as compared to CR2, and CR2 is red-shifted by ~140 nm as compared to SQ2. Same trends were observed for SQ3, CR3 and RH3 (Supplementary Data, Fig. S1).

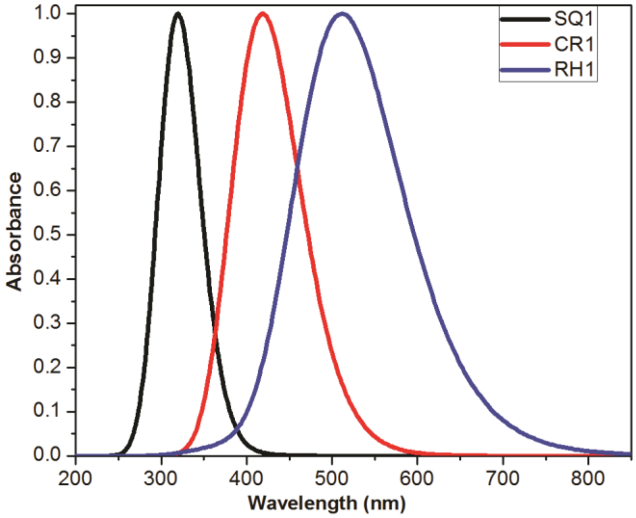

Fig. 4 — Calculated absorption spectra for SQ1, CR1 and RH1.

SAC-CI

Symmetry Adopted Cluster Configuration Interaction (SAC-CI) is a cluster expansion method which converges more rapidly than the Configuration Interaction (CI) method. SAC-CI examines the singly and doubly excited states which mix up with the ground and the targeted excited states[33-37]. The singlet geometries of SQ molecules obtained at B3LYP/6-311+G(d, p) level deal with SAC-CI calculations with 6-31+G(d) basis set. Since SAC-CI predicts electronic excitations more accurately than TDDFT in the case of neutral squaraines and croconines, herein we have used SAC-CI as one of the methods to predict electronic excitations. SAC-CI calculations have been performed with Level 2 and Window option[31-32,38-39]. SAC-CI calculated results of squarate, croconate and rhodizonate dianions are in good agreement with experimental excitation energies and are shown in Table S3 (Supplementary Data).

The experimental absorption for SQ2 is observed at 381 nm, and the TD-DFT calculated absorption is at 346 nm. The SAC-CI calculated absorption (390 nm) is in good agreement with experimental excitation energy (shown in Table S3). The major transition

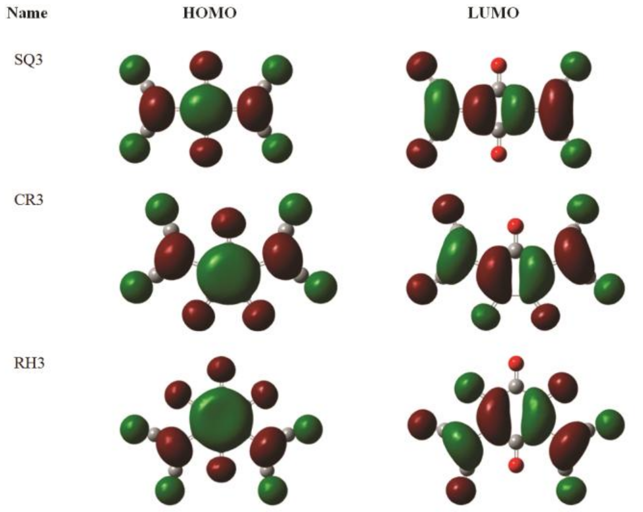

Fig. 5 — FMOs of SQ3, CR3 and RH3.

from HOMO to LUMO and other contributions are also shown in Table S3 (contributions of C_i coefficient more than 0.08 are tabulated).

Frontier molecular orbitals

Frontier molecular orbitals (FMO) were generated by population analysis with 6-311+G(d, p) basis set at B3LYP level. FMOs of SQ3, CR3 and RH3 dianions are shown in Fig. 5. FMOs of other molecules are given in Table S4 (Supplementary Data). The HOMO and LUMO energies of molecule SQ1 are 2.22 eV and 5.96 eV respectively and their corresponding HOMO-LUMO gap is 3.74 eV (shown in Table 4). On changing the central four-member ring with five-member ring, i.e., molecule CR1, both HOMO and LUMO levels get stabilized, but stabilization of LUMO is larger as compared to HOMO, which results in a decrease in HOMO-LUMO gap. For the CR1 molecule, HOMO and LUMO energies are 1.75 eV and 4.56 eV respectively and the corresponding HOMO-LUMO gap is 2.81 eV. Further stabilization of HOMO and LUMO levels was observed when the central five-member ring is replaced with a six-member ring. In the case of molecule RH1, HOMO and LUMO energies of RH1 are 1.42 eV and 3.55 eV respectively and their HOMO- LUMO gap is 2.13 eV. This decrease in HOMO-LUMO gap is due to change in the central ring that leads to stabilization of HOMO and LUMO levels. A similar trend is followed by SQ2, CR2 and RH2 (Fig. 6). In a similar way, there is a decrease in the HOMO-LUMO gap from SQ3 to CR3 to RH3. The change in central four-member ring with a five-member ring and five-member ring with the six-member ring results in the stabilization of HOMO and LUMO levels. It is clear that red-shifted absorption in RH dianion derivatives as compared to the corresponding CR dianion derivatives is due to stabilization of HOMO and LUMO levels (CR dianion derivatives also shows red-shifted absorption as compared to corresponding SQ dianion derivatives) (see Supplementary Data, Fig. S2).

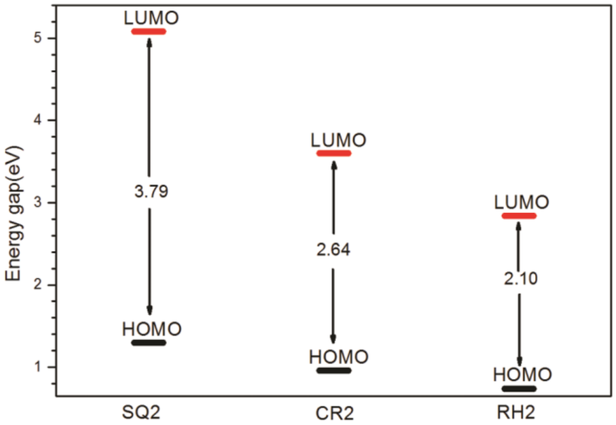

Fig. 6 — Stabilization of HOMO and LUMO showing decrease in HOMO-LUMO gap SQ2, CR2 and RH2.

Charge transfer also been evaluated for all the molecules with TDDFT method. In most of the cases Oxygen act as a donor while central ring as acceptor. However, there is no general trend is observed, as charge transfer depends on a number of substituents on central ring (Table S5).

Conclusions

The squarate (SQ1-SQ3), croconate (CR1-CR4) and rhodizonate (RH1-RH7) dianion derivatives are studied by increasing the number of substitutions of dicyanomethylene group on the central ring with the help of density functional theory, time dependent density functional theory and SAC-CI methods. The introduction of a dicyanomethylene group in squarate croconate and rhodizonate results in an increase in absorption of the molecule and a further increase in the number of dicyanomethylene groups further increases the absorption maxima. Dianions RH7, RH3 and RH1 with three, two and one substituted dicyanomethylene groups respectively show absorption at 739 nm, 603 nm and 521 nm respectively. The calculated absorption maxima for SQ3, CR3 and RH3 are 395 nm, 493 nm and 603 nm respectively, which shows that absorption energies of molecules depend largely on the size of the central ring and central angle. On increasing the size of the central ring from four-member to five-member and from five-member to six-member, a red-shift of ~100 nm is observed.

Supplementary Data

Supplementary data associated with this article are available in the electronic form at http://www.niscair.res.in/jinfo/ijca/IJCA_57A(8-9)1121-1127_SupplData.pdf.

Acknowledgement

CP thanks Council of Scientific and Industrial Research, New Delhi, India, for financial support (No. 02(0339)/18/EMR-II).

References

1 West R, Niu H Y, Powell D L & Evans M V, *J Am Chem Soc*, 82 (1960) 6204.
2 Lopes J G S, Oliveira L F C De, Edwards H G M & Santos P S, *J Raman Spectrosc*, 35 (2004) 131.
3 Ribeiro M C C, Oliveira L F C De & Goncalves N S, *Phys Rev B*, 63 (2001) 104303.
4 Ribeiro M C C, Oliveira L F C De & Santos P S, *Chem Phys*, 217 (1997) 71.
5 Ribeiro S J L, Goncalves R R, de Oliveira L F C & Santos P S, *J Alloys Compd*, 216 (1994) 61.
6 Oliveira L F C De, Mutarelli S R, Gonc N S & Santos P S, *Quím Nova*, 15 (1992) 55.
7 Ito M & West R, *J Am Chem Soc*, 85 (1963) 2580.
8 West R & Niu H Y, *J Am Chem Soc*, 85 (1963) 2586.
9 Glick M D, Downs G L & Dahl L F, *Inorg Chem*, 3 (1964) 1712.
10 Glick M D & Dahl L F, *Inorg Chem*, 5 (1966) 289.
11 Takahashi M, Kaya K & Ito M, *Chem Phys*, 35 (1978) 293.
12 Seitz G & Imming P, *Chem Rev*, 92 (1992) 1227.
13 Diniz R, De Sá L R V, Rodrigues B L, Yoshida M I & Oliveira L F C De, *Inorg Chim Acta*, 359 (2006) 2296.
14 Zhao B & Back M H, *Can J Chem*, 70 (1992) 135.
15 Fatiadi A J, *J Org Chem*, 45 (1980) 1338.
16 Fatiadi A J, *J Am Chem Soc*, 100 (1978) 2586.
17 Fabre P L, Dumestre F, Soula B, & Galibert A M, *Electrochim Acta*, 45 (2000) 2697.
18 Kamat P V, Fox M A & Fatiadi A J, *J Am Chem Soc*, 106 (1984) 1191.
19 Doane L M & Fatiadi A J, *Angew Chem Int Ed*, 21 (1982) 635.
20 Tripathi A, Promila & Prabhakar C, *J Phys Org Chem*, 30 (2017) 3673.
21 Fatiadi A J, *J Res Natl Bur Stand Sect*, 85 (1980) 73.
22 de Oliveira V E, de Carvalho G S & Yoshida M I, *J Mol Struct,* 936 (2009) 239.
23 *Gaussian 09*, *Rev. E.01*, (Gaussian, Inc., Wallingford, CT) 2013.
24 Lee C & Yang W, *Phys Rev B*, 37 (1988) 785.
25 Becke A D, *J Chem Phys*, 98 (1993) 5648.
26 Zhao Y & Truhlar D G, *Theoret Chem Acc*, 120 (2008) 215.
27 Becke A D, *J Chem Phys*, 98 (1993) 1372.
28 Yanai T, Tew D P & Handy C N, *Chem Phys Lett*, 393 (2004) 51.
29 Chai J D & Head-Gordon M, *Phys Chem Chem Phys*, 10 (2008) 6615.
30 Thomas A, Chitumalla R K, Puyad A L, Mohan K V & Jang J, *Comput Theoret Chem*, 1089 (2016) 59.
31 Prabhakar C, Yesudas K, Chaitanya G K, Sitha S, Bhanuprakash K & Rao V J, *J Phys Chem A*, 109 (2005) 8604.
32 Puyad A L, Prabhakar C, Yesudas K, Bhanuprakash K & Rao V J, *J Mol Struct* (*THEOCHEM*), 904 (2009) 1.
33 Nakjima T & Nakatsuji H, *Chem Phys Lett*, 280 (1997) 79.
34 Wan J, Ehara M, Hada M & Nakatsuji H, *J Chem Phys*, 113 (2000) 5245.
35 Nakajima T & Nakatsuji H, *Chem Phys Lett*, 300 (1999) 1.
36 Wan J, Hada M, Ehara M & Nakatsuji H, *J Chem Phys*, 114 (2001) 842.
37 Nakatsuji H, in *Computational Chemistry-Reviews of Current Trends*, Vol. 2, edited by J Leszczynski, (World Scientific, NJ, USA) 1997.
38 Puyad A L, Chaitanya G K, Prabhakar C & Bhanuprakash K, *J Mol Mod*, 19 (2013) 275.
39 Prabhakar C, Chaitanya G K, Sitha S, Bhanuprakash K & Rao V J, *J Phys Chem A*, 109 (2005) 2614.